

Automatic segmentation of gallbladder using bio-inspired algorithm based on a spider web construction model

V. Muneeswaran¹  · M. Pallikonda Rajasekaran²

Published online: 13 January 2018

© Springer Science+Business Media, LLC, part of Springer Nature 2018

Abstract In medical image processing, an accurate segmentation and classification are very important and this field still needs an effective computer-based algorithm for accomplishing the task. In gallbladder segmentation, only few automatic segmentation methodologies have been presented. The accuracy is very important in medical image processing for accurate diagnosis of the disease. In this paper, by exploiting the basic web building behavior of spiders, we developed a bio-inspired algorithm based on the spider web construction process for image segmentation process in medical images. The aim of this paper is to detect the shape of the gallbladder and to segment the gallstones and polyps located inside the gallbladder using a computer-based algorithm. It is necessary to apply a suitable preprocessing method in order to eliminate the irregularities presenting in the ultrasound scan images. In the preprocessing stage, histogram equalization and DooG filter are applied to enhance the contrast of the image. After that, the proposed spider web algorithm is applied in the segmentation process. The performance metrics of the proposed method are evaluated by implementing the proposed method to test the input dataset of 60 patients and it is compared with the results obtained from conventional segmentation methods. The values of DSC, OF, OV and PE for images with no lesions are 0.873167, 0.8389, 0.81705 and 0.81452.

✉ V. Muneeswaran
munees.klu@gmail.com

M. Pallikonda Rajasekaran
m.p.raja@klu.ac.in

¹ Department of Instrumentation and Control Engineering, Kalasalingam Academy of Research and Education, Anand Nagar, Krishnankoil, Srivilliputtur Post, Virudhunagar District, Tamilnadu 626126, India

² Department of Electronics and Communication Engineering, Kalasalingam Academy of Research and Education, Anand Nagar, Krishnankoil, Srivilliputtur Post, Virudhunagar District, Tamilnadu 626126, India

Keywords Gallbladder segmentation · Gallstone segmentation · Bio-inspired algorithm · Spider web construction

1 Introduction

In the computer-based diagnosis of human organs, the major task is the segmentation of the specific organ of the scanned image. After segmentation process, further investigations such as quantification and classification are done. The gallbladder is a small sac-like organ positioned at a lower level of liver which garners digestive fluid extruded from liver and emancipates it in the course of digestion. Naturally, the gallbladder is located in the right upper quadrant abdominal cavity. Usually the wall of gallbladder with clear edge looks like thin and glossy. Diagnosis of gallstones employing suitable imaging modality becomes conspicuous as it incites the malignant gall tumor. Ultrasound imaging modality is usually preferred on the grounds that it is noninvasive and non-ionizing. Figure 1 shows that the ultrasound scan images have an irregular background and the edges of the gallbladder are blurred or missed. Hence, the accurate segmentation of the gallbladder shape is still a difficult process as it requires efficient algorithms. The shape of bladder varies from person to person due to several reasons. Gallstones and polyps are the general pathological diseases presenting in the bladder. If the gallbladder diseases are detected at earlier stages, their growth can be hindered. Presently the active contour models are the increasingly used method to extract the shape of the organs from the ultrasound images. Many works [1–5] used are edge-based active contour models for the shape extraction. Still, it has some shortcomings that often it gives either the contracted shape or expanded shape when comparing with the original shape, due to its inflation and deflation force. Sometimes, one or more loop occurs due to the self-crossings of the contour. Though some algorithms [6, 7] were presented to detect the self-crossings in images and videos, they seem to be less

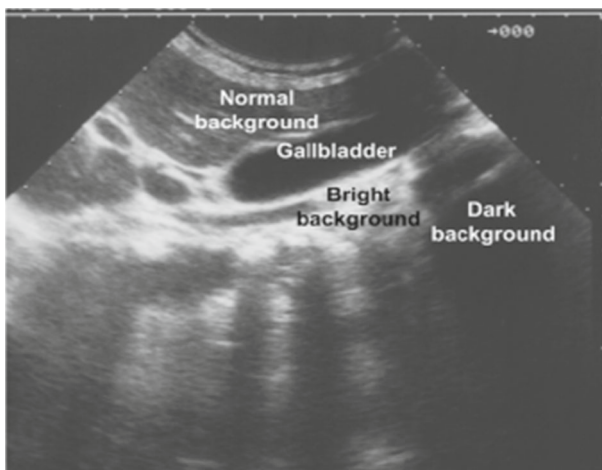


Fig. 1 Ultrasound scan image of the gallbladder

effective in medical image processing. Many works [8–13] have been proposed to segment the shape of the gallbladder.

To propose an accurate segmentation algorithm to extract the gallbladder (GB) and gallstone regions or other lesions, the below three sets of information must be taken into account. They are the position of the gallbladder in the ultrasound scan, place of the ultrasound source and information regarding the angle from which the gallbladder is scanned. Image segmentation is the process of partitioning the images into several regions based on the pixel values. The aim of this paper is to detect the shape of the gallbladder and to segment the gallstones and polyps located inside the gallbladder using a computer-based algorithm. It is necessary to apply a suitable preprocessing method in order to eliminate the irregularities presenting in the ultrasound scan images. A biologically inspired algorithm is presented in this work which is based on the spider web construction.

2 Related works

In this section, the previous works involved in gallbladder segmentation are discussed. Moreover, various bio-inspired algorithms are discussed along with their application to various problems as well as to image processing. Ciecholewski [9] has used active contour models to segment the gallbladder with lesions or without lesions. The active contour models such as membrane and motion equation and the gradient vector flow model (GVF snake) are employed to determine the edges of gallbladder, polyps or other changes. Then, the section of the image found on the outside of the segmented gallbladder is removed from the image. From the experimental results obtained from testing 600 ultrasound images, the dice similarity coefficient (DSC) is obtained for the three different active contour models employed in the paper. The average DSC for these three active contour models is 81.8%. In their work, histogram transformation is applied as the first step to enhance the contrast of the image. Then in 2011 [10], Marcin Ciecholewski applied the AdaBoost (adaptive boosting) and support vector machine (SVM) to locate and classify the lesions in the gallbladder as lithiasis or polyps. The performance is analyzed from the simulation results, and it is observed that the accuracy of 91% is obtained in classifying lithiasis only, 80% is obtained in classifying polyps and 78.9% is obtained in classifying the regions with both polyps and lithiasis. In the paper [8], Ogiela and Bodzioch have segmented gallbladder by employing two methods. They have employed binarization, binary image filtering with rank filter and contour identification. In the second method, the edges are detected by using histogram analysis. This method may provide wrong results when the polyps or gallstones are bright in the background of the dark region (gallbladder) and when they are presented next to the bladder edges. Xie et al. [13] have proposed a method for segmenting gallbladder using level set model. The results of the paper [9] are not evaluated with more scan images, and it provides better results of gallbladder without lesions. Hence, to improve the work, Marcin Ciecholewski has presented another work by using two active contour models which are edge-based model and region-based model. In this work, self-crossings and loops are removed using suitable methods and inflation force is dampened. By implementing histogram normaliza-

tion transformation and the Gaussian filter smoothing process, the image contrast is enhanced and the noises are removed. Then the edges of the gallbladder that fall on the dark background of the images are computed manually to initialize the contour. Subsequently the detected edge is smoothed by exploiting a convex hull algorithm. Lian et al. [12] have proposed automatic segmentation algorithm for gallbladder and gallstone from the ultrasound image. This work is accomplished in five stages. In the first stage, the authors employed Otsu thresholding process and anisotropic diffusion process in the preprocessing stage. The Otsu method extracts the weak edges presenting in the inner part of the gallbladder. The second stage which is the fine segmentation of the gallbladder is obtained using a global morphology filtering process. In the third stage, high-intensity regions such as gallstones are extracted using a parameter-adaptive pulse-coupled neural network (PAPCNN). A modified region growing model is employed in the next stage in order to avoid over segmentation of gallstones. The locally weighted regression smoothing process is applied as the final stage to obtain smoothed regions of the resulting regions. The authors tested the proposed work and compared the accuracy of the proposed with the previous works.

In paper [14], the authors presented a snake-based approach as a semiautomatic segmentation technique to apply on ultrasound images. The authors encompass the fly learning of statistical boundary models in this work without affecting the straight forward propagation of snakes. They analyzed the proposed algorithm to segment the in vivo ultrasound images. This method performs computation at low cost and requires less manual interaction. Wimmer et al. [15] proposed a segmentation method to segment cavity regions from ultrasound images. In this work, the authors located an arbitrary seed point inside the cavity and projected a equispaced radii from that location to the edge of the cavity. The distance between the seed point and the cavity edge is determined from the traces of a moving object. The contour is then segmented with the application of interacting multiple model (IMM) estimator along with a probabilistic data association filter (PDAF). This method does not contain any numerical optimization; hence, it shows less convergence rate. Abolmaesumi et al. [16] proposed a probabilistic active shape model to extract liver from the 3D scan image and this method is developed based on the nonparametric density estimates. A nearest neighbor boundary appearance model is combined with a series of boosted classifiers to obtain region information and used along with a shape model based on Parzen density estimation. The work reported in [17] is the first work to present the fully automatic gallbladder segmentation and they implemented volumetric analysis in volume information of non-contrast-enhanced and secretin-enhanced magnetic resonance (MR) cholangiopancreatography (MRCP) sequences. Initially a gallbladder outline space is engendered to develop 3D gallbladder shape features. Then these features are joined with 2D features in a support vector machine (SVM) classifier to locate gallbladder regions in MRCP volume data. Fine segmentation is obtained by a region-based level set approach. Volumetric analysis is performed for both sequences to calculate gallbladder volume differences between both sequences. In Saito et al. [18] reports joint optimization for segmentation and shape priors to overwhelm inter-subject variability in the place of a human organ. The authors presented a fast approximation for optimization. The performance of the proposed approximation is evaluated in the framework of gallbladder segmentation from a non-contrast computed tomography (CT) volume.

At first, the spatial standardization is applied and the posterior probability of the target organ is computed. Then simultaneous optimization of the segmentation, shape and location priors is accomplished with the help of a branch-and-bound method. Fast approximation is obtained by jointly using sampling technique in the eigenshape space to decrease the number of shape priors and an efficient computational method for computing the lower bound. To meet out the limitations of the above-said works, in this paper a spider web-based segmentation technique is presented.

The biologically inspired algorithms (BIA) are exposed to be the tremendous methods in many fields of engineering design, industrial optimization, networking, image processing, power system optimization and medical signal analysis [19–22]. Many works have been performed in the research field of BIA from the last decade twentieth century. Many such algorithms have been developed for last two decades and still there is a vast space for the engineers since some of them yield better solutions to only certain problems; not for all. Various bio-inspired algorithms involving swarm-based models and migration-based models are listed in Fig. 2. These algorithms are utilized in many industrial processes and research works for solving the optimization problems. They are particle swarm optimization (PSO) [23], ant colony algorithm [24], artificial bee colony [25], termite algorithm [26], artificial fish swarm algorithm [27], monkey search [28], cuckoo search [29], firefly algorithm [30], gray wolf optimizer [31], lion hunting algorithm [32], pigeon inspired algorithm [33], whale optimization [34], dragonfly algorithm [35], coral reef optimization algorithm [36] and more. Various conventional BIAs and species from which the algorithms are inspired are listed in Fig. 2. The gray wolf optimization (GWO) algorithm is inspired by the leadership and hunting process of gray wolves. This algorithm is first developed by Seyedali Mirjalili [31] to solve engineering design problems. In this algorithm, the three phases (searching for prey, encircling prey and attacking prey) involved in the hunting process of wolves are applied. The authors analyzed the performance of the gray wolf algorithm by implementing it in three design problems: designing compression spring, designing welded beam and designing a pressure vessel. In [32], a population-based algorithm inspired from the lion is proposed. The cooperation characteristics of the lion are exploited, and algorithm is developed for optimization problem. Seyedali Mirjalili in another work [35] presented a dragonfly optimization algorithm along with its two versions namely, binary DA (BDA) and multi-objective DA (MODA). MODA is implemented in designing the submarine propeller and its performance is evaluated. Salcedo-Sanz et al. [36] developed coral reef optimization algorithm by inspiring from the reproduction and fight for space mechanisms in the coral reef. The algorithm is validated by implementing in the mobile network application and designing wind farms.

By adopting the behavior of spider species, social spider algorithm is presented in many works to solve various optimization problems such as economic load dispatch problem [37] and fault diagnosis in power distribution network [38]. Anter et al. [39] presented a novel feature selection approach for detecting tumor from a CT liver image by implementing the social spider optimization algorithm. This algorithm detects the optimal region of the search space based on the interaction of individual species in the colony. The optimal region refers to the necessary feature set to be selected from a large feature set. The performance of the work is analyzed from the metrics such as

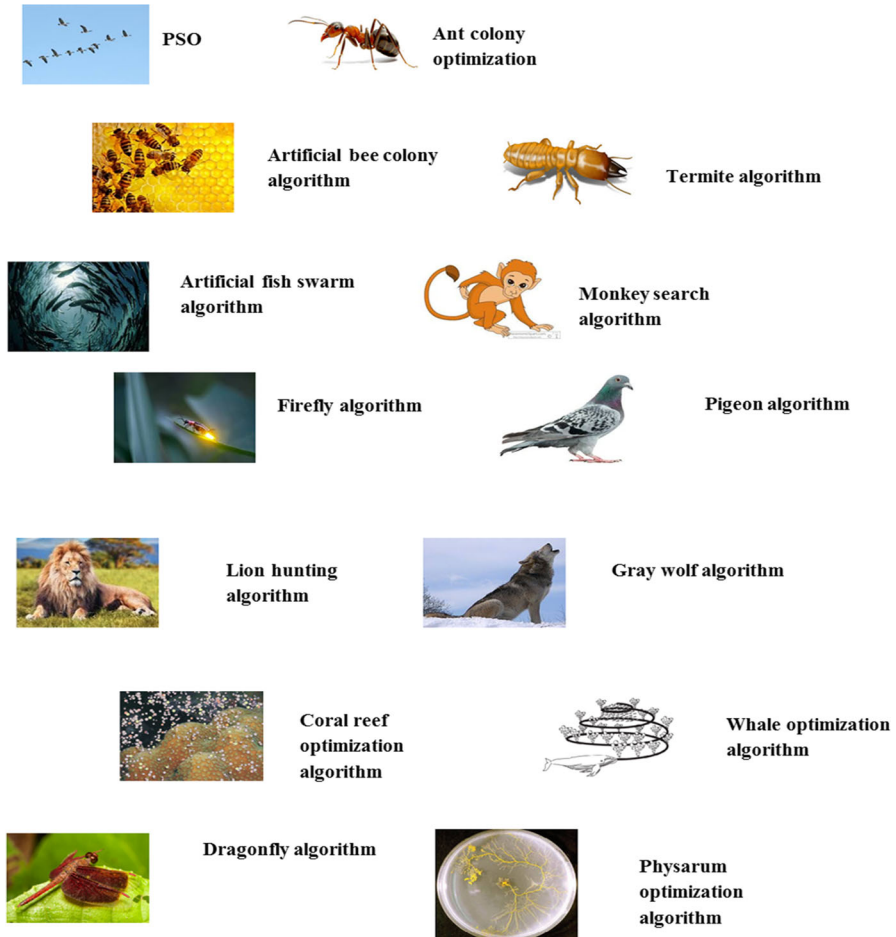


Fig. 2 Bio-inspired algorithms

confusion matrix, precision, recall and accuracy. In paper [40], multi-level thresholding segmentation using two bio-inspired algorithms is presented. The two algorithms are flower pollination (FP) which is inspired by pollination process in flower and the social spiders optimization (SSO) algorithms. Initial solutions (threshold values) are first produced by a histogram. Then the optimal threshold values are computed using the between-class variance or Kapur's method.

3 Proposed bias method

The ultrasound scan images obtained from eight patients are taken as input images for analyzing the proposed method. In the first step, in order to improve the quality of the image, histogram equalization process and difference of offset Gaussian (DooG) filter are applied as the preprocessing methods. After enhancing the image, it is processed

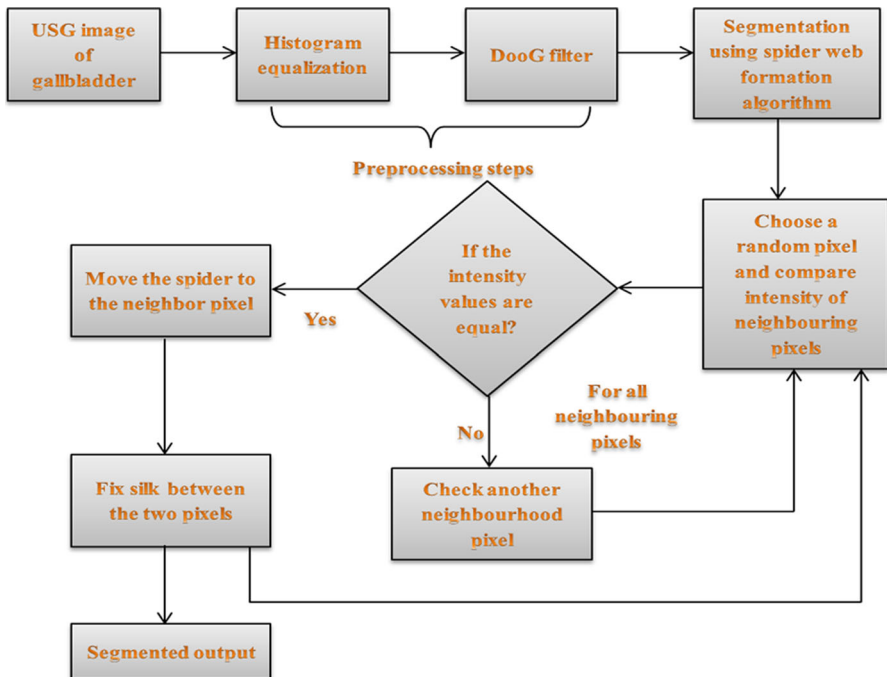


Fig. 3 Steps involved in the proposed work

for segmenting the gallbladder region by applying bio-inspired spider web formation algorithm. The various processes involved in this work are illustrated in Fig. 3.

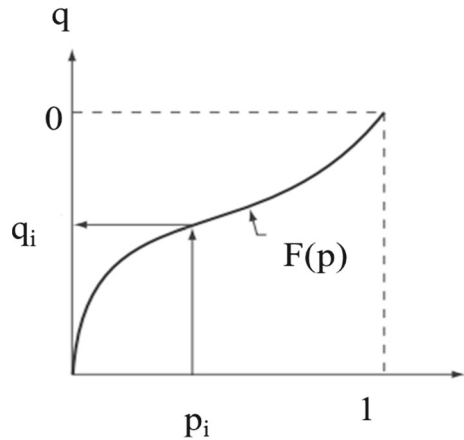
3.1 Histogram equalization (HE)

Histogram equalization (HE) is the technique used to increase the contrast of the image so that the image visibility can be improved without altering the structure. In this method, the information contained in an image is associated with the probability of the incidence of each gray level. To increase the information contained by the image, the histogram transformation is employed to homogeneously redistribute the above-said probability factor.

To define the histogram of an image, A , at first let us consider that B is the output image obtained from HE process and p and q are the gray levels of A and B , respectively. The gray levels in these images are always in the range of values between 0 and 1. $H(p)$ and $H(q)$ represent the normalized histogram of images A and B . It can also be known as the gray-level probability density functions (PDFs). For every gray level of image A , (p_i) , the transformation function (Fig. 4) shown in Eq. 1 produces a new gray value (q_i) .

$$q = F(p) \quad (1)$$

Fig. 4 Single-valued, monotonically increasing transformation function



The function $F(p)$ must obey two constraints that it should be single-valued and monotonically increasing in order to maintain the intensity order in the transformed image as in the input image and the function should fall in the range from 0 to 1. For the transformed variable q , the histogram function or PDF can be obtained from Eq. 2. This transformation is known as histogram equalization.

$$H(q) = \left[H(p) \frac{dp}{dq} \right] \quad (2)$$

When $H(q) = 1$, Eq. 2 becomes

$$dq = H(p) dp \quad (3)$$

and hence

$$q = F(p) = \int_0^p H(w) dw \quad (4)$$

Equation 4 represents the cumulative distribution function (CDF) of gray level, p , of the image.

Equation 5 denotes the probability of incidence of gray level p_i in the image A is represented by

$$H(p_i) = \frac{n_i}{n} \quad (5)$$

where n is the total number of pixels in the image and n_i the number of pixels with gray level p .

3.2 DooG filter

In order to enhance the edges in the image, the DooG filter is applied. The output image obtained from histogram equalization is given to the DooG filter. The purpose of filter is to remove noise in the image before applying segmentation process. Noise elimination is an essential task in medical image analysis [41,42]. The DooG filter highlights the edges by producing maximum absolute pixel value for the pixels occurred in an edge. Pixels occurred in the edge is appeared as a sharp gradient between the pixels in the actual image with a definite direction. The magnitude and orientation are computed from the first derivative of the gradient in horizontal and vertical axis. The DooG filter is implemented in this work by reason of its very less computation time. Thus it lessens computational cost. A 2D isotropic Gaussian function is represented as

$$\mathbb{G}(x, y) = \frac{1}{\sqrt{2\pi}\sigma} e^{-(x^2+y^2)/2\sigma^2} \quad (6)$$

The first derivative of GF in horizontal axis is given in

$$\mathbb{G}'_{\sigma}(x, y) = \frac{\partial \mathbb{G}_{\sigma}(x, y)}{\partial x} = \frac{-x}{\sigma^2} \mathbb{G}_{\sigma}(x, y) \quad (7)$$

The difference of offset Gaussian (DooG) in the horizontal axis is represented in Eq. 8.

$$\text{DooG}_{\sigma}(x, y) = \mathbb{G}_{\sigma}(x, y) - \mathbb{G}_{\sigma}(x + \delta, y) \quad (8)$$

δ is offset between centers of two Gaussian kernels. The DooG function along various directions can be computed by revolving the functions of Eqs. 7 and 8.

$$\mathbb{G}'_{\sigma,\alpha}(x, y) = \mathbb{G}'_{\sigma}(x \cos \alpha + y \sin \alpha, -x \sin \alpha + y \cos \alpha) \quad (9)$$

$$\text{DooG}'_{\sigma,\alpha}(x, y) = \text{DooG}'_{\sigma}(x \cos \alpha + y \sin \alpha, -x \sin \alpha + y \cos \alpha) \quad (10)$$

The direction can be determined by computing the edge energy. The edge energy of a Gaussian smoothed image $Z_{\sigma}(x, y)$ at a point, p , is denoted as $E(p, \alpha)$. It is the magnitude of the gradient of the image in the direction α .

$$E(p, \alpha) = |Z(x, y) * \mathbb{G}'_{\sigma,\alpha}(x, y)| \quad (11)$$

There are two feasible directions depending on the edge energy (forward and the backward).

3.3 Spider web-based segmentation

Biologically inspired design (BID) and algorithm utilize equivalent biological event or a habitant to obtain solutions to engineering problems [43–47]. Many products have been manufactured based on the biologically inspired designs. In the field of developing algorithms for accomplishing a particular task, biologically inspired algorithms

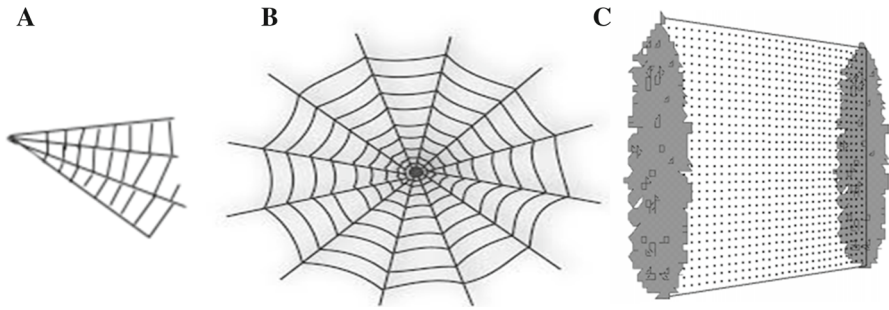


Fig. 5 Spider web, **a** sheet web, **b** orb web, **c** hypothetical vertical web

(BIA) have been derived by studying the behavior of group of insects, animals and others. The spider web algorithm is applied in this work for segmenting the bladder and gallstone or other lesions presenting in the scan image. This algorithm is inspired from the behavior of spider in constructing cobweb.

Generally the spider species construct web for catching its prey. The spider web is built by the spider silk, which is thrust out from its spinnerets. Every spider has some spinneret glands and each gland is able to produce spider silk. The diameter of silk in the spider web is in the range of 0.02–0.15 mm. The spider web becomes visible to human eye due to the reflection of light on the silk. A spider with a body length of 5 mm can build a web for a volume of 100 m³. Spider web can be built in vertical or horizontal planes. There are many kinds of spider web. Of them, orb web is built in the vertical plane and sheet web is built in the horizontal plane. Figure 5 shows sheet web, orb web and a hypothetical, vertical web built between two plants. In web construction, the spider first creates a sticky silk thread and thrust it out in the air to stick onto a suitable place. Then the spider moves along the thread to the fixed place and adds a thread to provide more strength to the thread. Then it again comes back to the original position and builds other threads to form a web. The different kinds of webs such as orb web, cobweb and sheet web can be constructed based on the type of spider and based on the approach of silk fixing.

By exploiting this basic web building behavior of spiders, we developed a bio-inspired algorithm based on spider web construction process for image segmentation process in medical images. This paper explicits the proposed algorithm to segment the gallbladder region. As the preprocessing step, histogram equalization is applied to enhance the contrast of the image. After that, the proposed spider web algorithm is applied in the segmentation process. The accuracy of the proposed method is evaluated and it is compared with the results obtained from other segmentation methods.

In digital image processing an image, I is represented as an $n \times m$ matrix of pixel values. The given image is preprocessed using histogram and DooG filter. The output image of the DooG filter is then segmented using the spider web algorithm. In spider web construction, the spider first creates a sticky silk thread and thrust it out in the air to stick onto a suitable place. Then the spider moves along the thread to the fixed place and adds a thread to provide more strength to the thread. Then it again comes back to the original position and builds other threads to form a web. By adopting

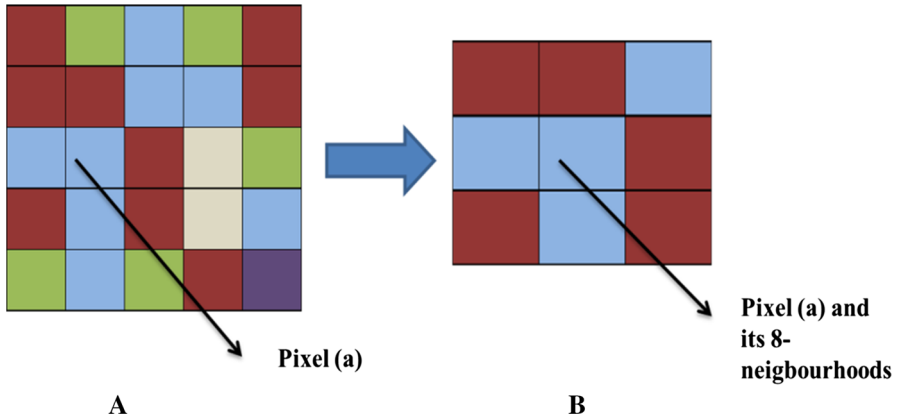


Fig. 6 Pixel representation of **a** pixels of the image with the randomly chosen pixel **(a)**, **b** neighboring pixels of pixel **a**; various colors in the image represent various pixel values (color figure online)

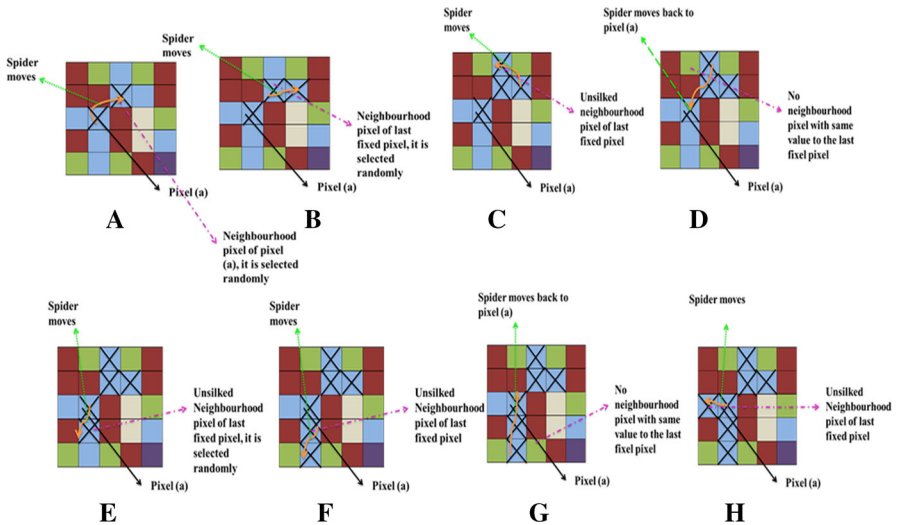


Fig. 7 Steps in spider web-based segmentation. **a** Initial spider location and its movement to the next pixel are shown. **b** Last fixed pixel moves to its neighborhood pixel with same color (intensity). **c–h** Same process as in **b** happen (color figure online)

this principle behind web construction, the pixels are segmented in the image. Image pixels are considered as the spider’s location. Initially a pixel is selected randomly as a spider [pixel (a)]. Then from that location, spider web construction begins. The initial pixel checks all of its eight neighboring pixels in the image. It chooses the neighboring pixels whose intensity value is equal to that of pixel (a). These pixels are denoted as set *X*. It is similar to the process of sticking the silk thread in a suitable place. Figure 6 represents the various pixels of the image and the chosen pixel and its neighborhood pixels are also represented.

When the neighboring pixels with same intensity values are selected, the spider moves from its initial position to one of the unsilked neighboring pixels in set X . The silked pixel must not be considered. After moving to the next pixel, silk fixing process is performed. The thread between two pixels represents that they are connected. After silk fixing, the next move is started from the last fixed pixel. If the neighboring pixel is of different intensity value, the spider comes back to the initial position and checks another neighboring pixel and this process continues when all the pixels in the set X are checked for silk fixing process. The segmented region is represented by the set of silked pixels. The working procedure of image segmentation process under spider web construction algorithm is shown for the example of pixel matrix of image shown in Fig. 6 are illustrated in Fig. 7. The same colored box represents the pixels having same intensity values. The silked pixels (boxes in figure) are marked with 'X.' Figure 7 shows that the pixels having same intensity values are silked. Hence, the region with same colored pixels can be segmented with this method effectively.

Algorithm -1: Spider web based segmentation

1. Choose a random pixel in the ROI as a spider (pixel (a))
 2. Compute the intensity of the pixel (intpixel(a)) and assign it to P.
 3. Compute the intensity of its neighborhood pixels (intneighpixel(a)) and assign it to Q.
 4. **while** (i<size(Q))
 5. Compare P and Q[i]
 6. **if** P=Q, **do**
 7. Move (a, neighpixel (a)) // move the spider to the neighbor pixel
 8. fixsilk (Position (a), Position (neighpixel (a))) // fix silk between the two pixels
 9. Lastfixed pixel (a) \leftarrow neighpixel(a)
 10. Increment i by 1 and **goto** step-5
 11. **else**
 12. Move (Lastfixed pixel (a), pixel(a))
 13. **end if**
 14. **end while**
 15. **Goto** step-3
-

4 Experimental results

The ultrasound scan images of gallbladder with no lesions and with gallstones are taken for evaluating the proposed method. The proposed spider web-based segmenta-

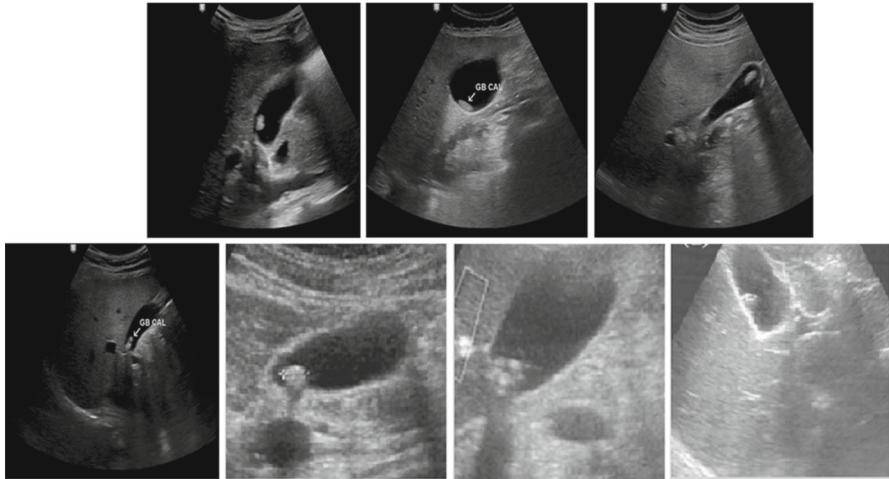


Fig. 8 Input images with gallstone (input set 1)



Fig. 9 Output images of the set of input images in Fig. 8

tion algorithm in this paper was executed in MATLAB software (version: 8.0.0.783, R2012b) on a computer equipped with Intel® Core™ i5-2410M processor of 2.30 GHz clock speed and 8 GB RAM to evaluate the results. The input ultrasound images are shown in Fig. 8. These scan images of 60 patients were collected from a private diagnostic center located in the Rajapalayam city of India. As it is superfluous to tabulate results for 60 patients, we have taken the mean values of parameters obtained for those images in order to test and validate the performance of the proposed method. In Fig. 9, the output images obtained using spider web-based segmentation algorithm are shown. Figure 8 shows seven input images having gallstone. Figure 10 shows the gallbladder images which have no any lesions, and Fig. 11 shows the corresponding output

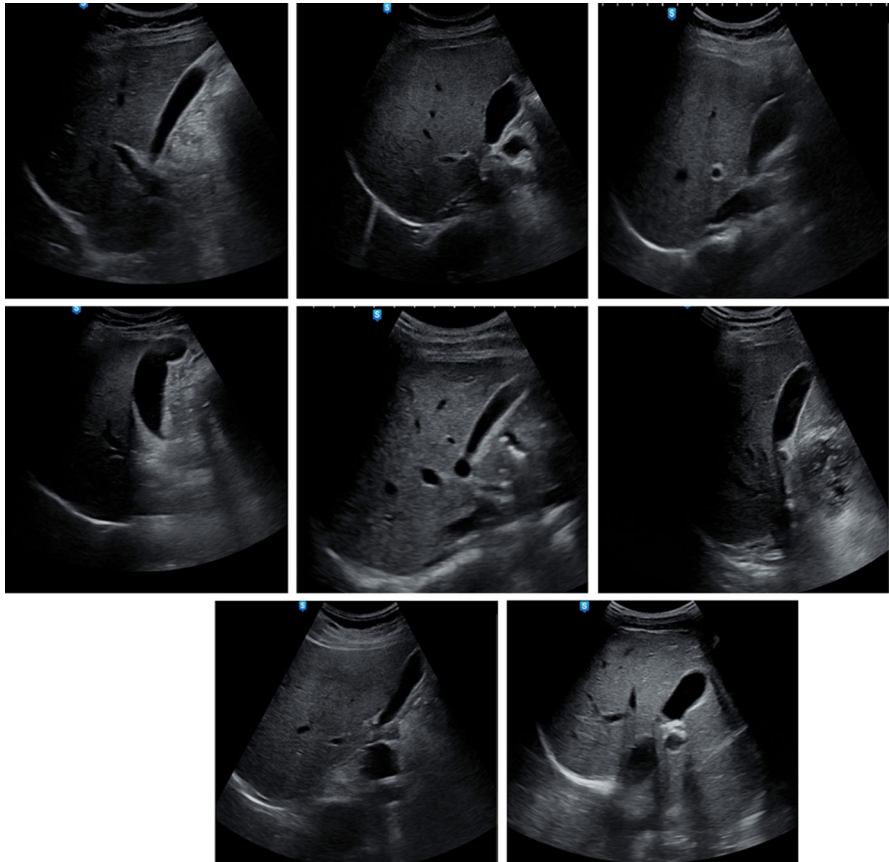


Fig. 10 Images with no lesions (input set 2)

images. These images are analyzed and the performance metrics are listed in tables and mean values are computed to compare with previous works. The input images are also examined with other state-of-the-art methods such as GVF snake model, snake balloon, parameter-adaptive pulse-coupled neural network, modified edge-based model (ME) and modified morphological model (MO), which are listed in the works [11, 12]. The performance metrics are also computed using these methods and the mean values are tabulated for comparison.

Initially the histogram equalization is performed to get a clear image which is a contrast enhanced image. Usually in the medical images there exist several noises which show a severe impact on results. Noises may lead to false diagnosis. They are instrument noise, Gaussian noise, physiological noise and thermal noise. In this work, we employed DooG filter to remove the noise in the preprocessing step. The reason for choosing this filter is because of its faster performance. Then the proposed segmentation process is applied to segment the gallbladder as well as the gallstone area from the image.

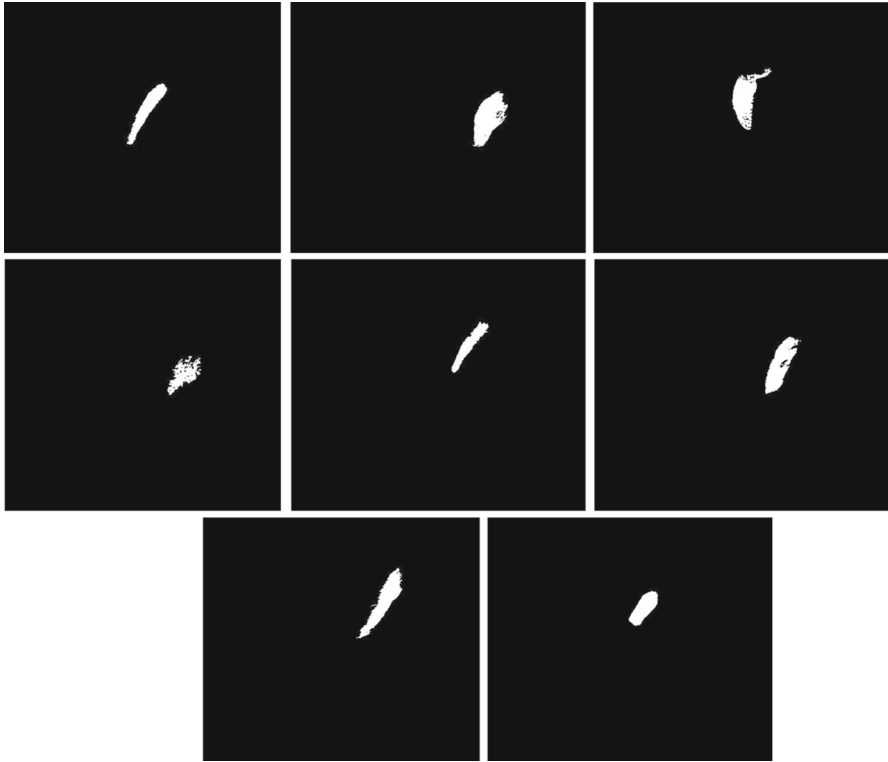


Fig. 11 Output images of the set of input images in Fig. 10

The computed parameters are dice similarity coefficient (DSC), overlap function (OF), overlap value (OV) and position error (PE). The first three parameters find out the similarity between two regions (automatic segmented output and manually segmented gallbladder region). Position error represents the error between two regions which can be obtained by Eq. 15.

$$\text{DSC} = 2 \times \frac{|S_1 \cap S_2|}{|S_1 + S_2|} \quad (12)$$

$$\text{OF} = \frac{|S_1 \cap S_2|}{S_2} \quad (13)$$

$$\text{OV} = \frac{|S_1 \cap S_2|}{|S_1 \cup S_2|} \quad (14)$$

S_1 group of pixels in manually segmented region. S_2 group of pixels in automatic or semiautomatic segmented region.

$$\text{PE} = \frac{1}{2c} \sum_{i=1}^c \text{dist}(u_i, v) + \frac{1}{2d} \sum_{j=1}^d \text{dist}(u, v_j) \quad (15)$$

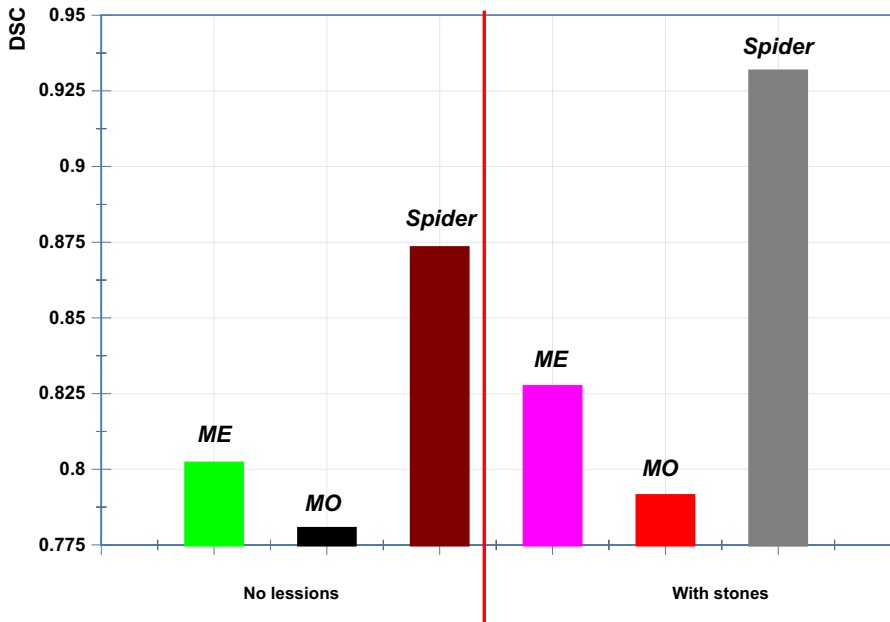


Fig. 12 Comparison of DSC for images with gallstones and with no any lesions

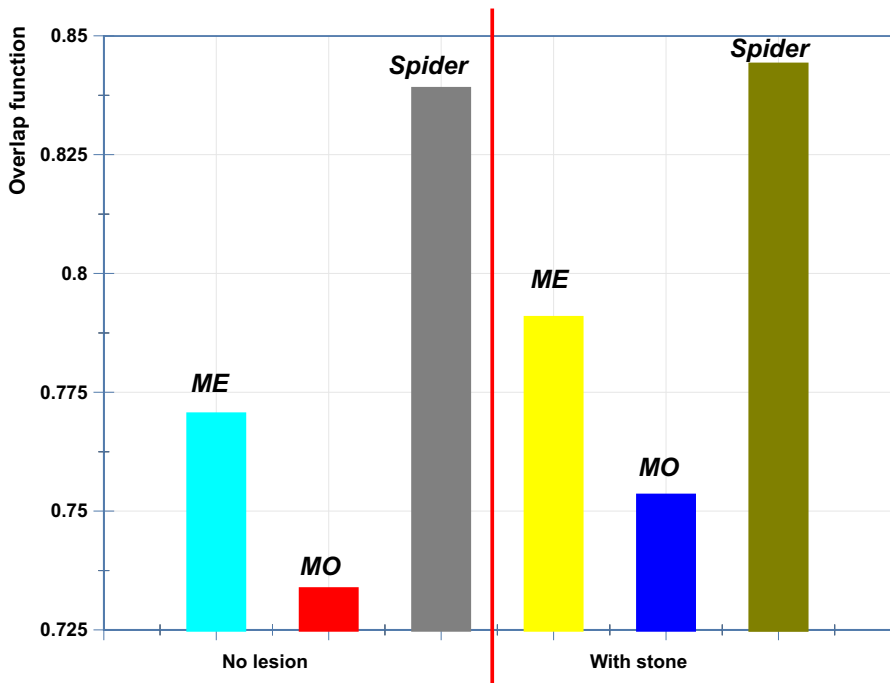


Fig. 13 Comparison of overlap function for images with gallstones and with no any lesions

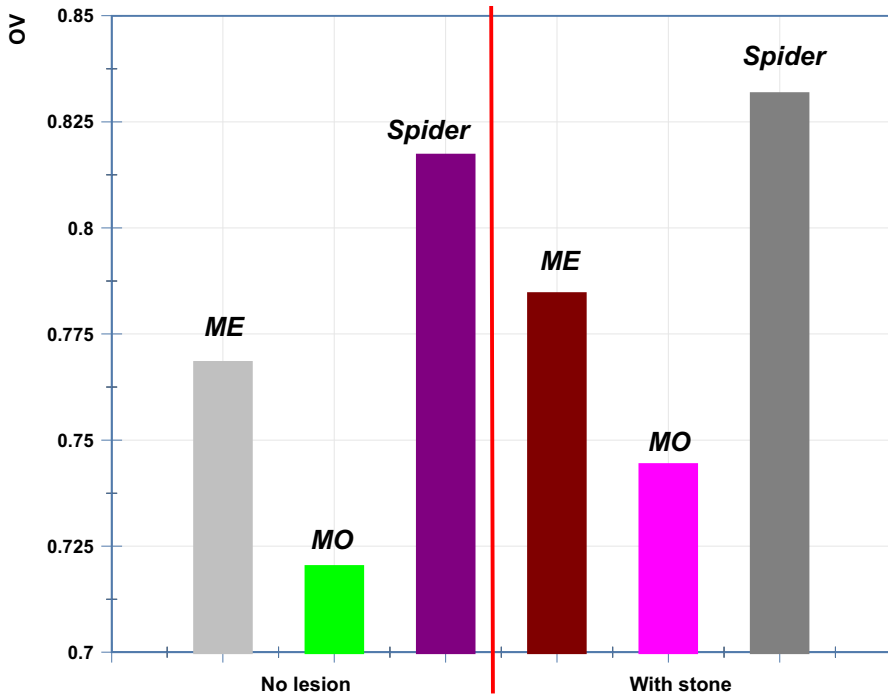


Fig. 14 Comparison of overlap value for images with gallstones and with no any lesions

u group of c number of pixels of the region to be compared, v group of d number of pixels of the region to be compared, $\text{dist}(u_i, v)$ —shorter distance between the pixel u_i and every pixel of the region v . $\text{dist}(u, v_j)$ —shorter distance between the pixel u and every pixel of the region u_j .

The performance metrics are evaluated and listed in Tables 1, 2 and 3. Table 1 gives the metrics for the two sets of input images applied in the work (with gallstones and image without any lesions). For the images having gallstones in the gallbladder, the parameters are computed separately for gallbladder region and gallstone region. Table 2 compares the performance metrics of the proposed method with other conventional methods for image with stone and without any disease. In this table, the mean values are denoted. In Table 3, the metrics of the gallbladder with gallstones are computed separately for bladder region and stone region. Similarly, these values obtained for the proposed method are compared with the conventional methods (Figs. 12, 13, 14, 15, 16, 17, 18, 19). In the proposed method, the measurements of DSC, OF, OV and PE for gallbladder with stone are 0.9315, 0.843971, 0.831529 and 0.839086, respectively. It is seen that the values of metrics such as OF, OV and DSC are less in the proposed method closer to the value '1' in the proposed method when compared with the other methods. Besides, the value of PE metric is closer to the value '0' in the proposed method when compared with the other methods. Moreover, to validate the performance of DooG filter in this work, the proposed method is compared with other filters such as moving average filter, Gaussian filter and Sobel filter. The results are tabulated in Table 4.

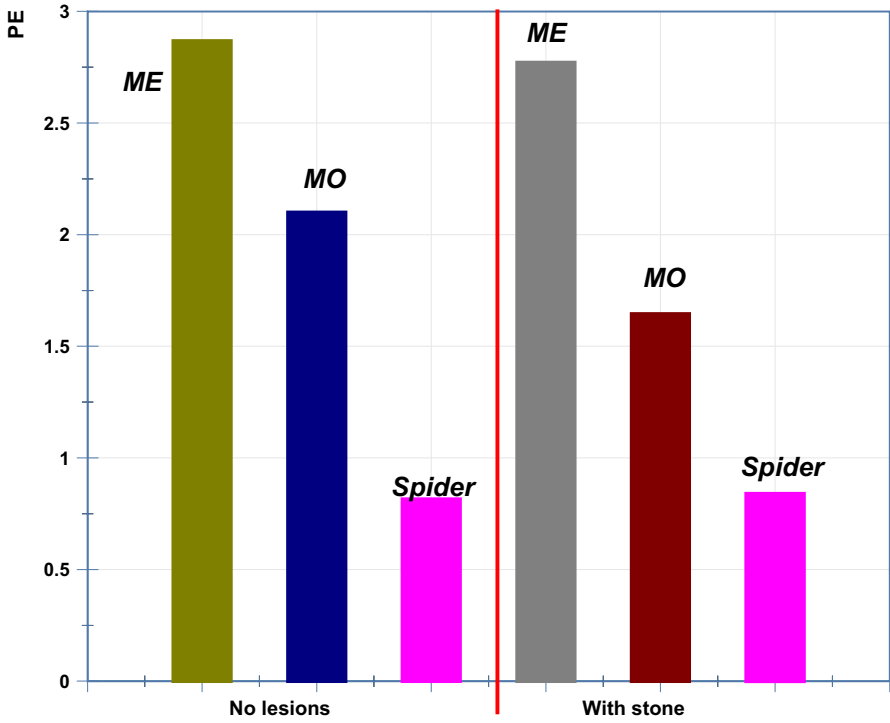


Fig. 15 Comparison of position error for images with gallstones and with no any lesions

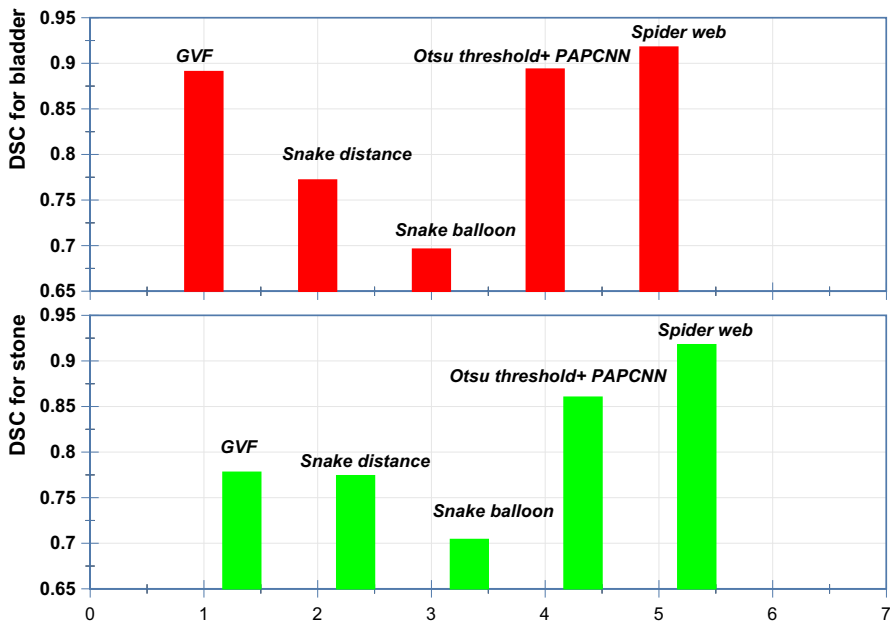


Fig. 16 Comparison of DSC for images with gallstones

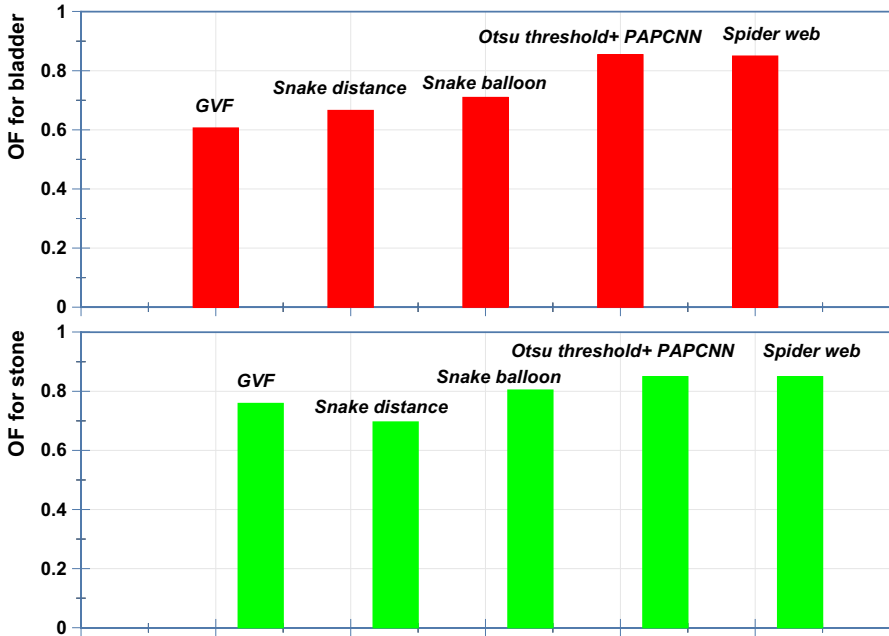


Fig. 17 Comparison of OF for images with gallstones

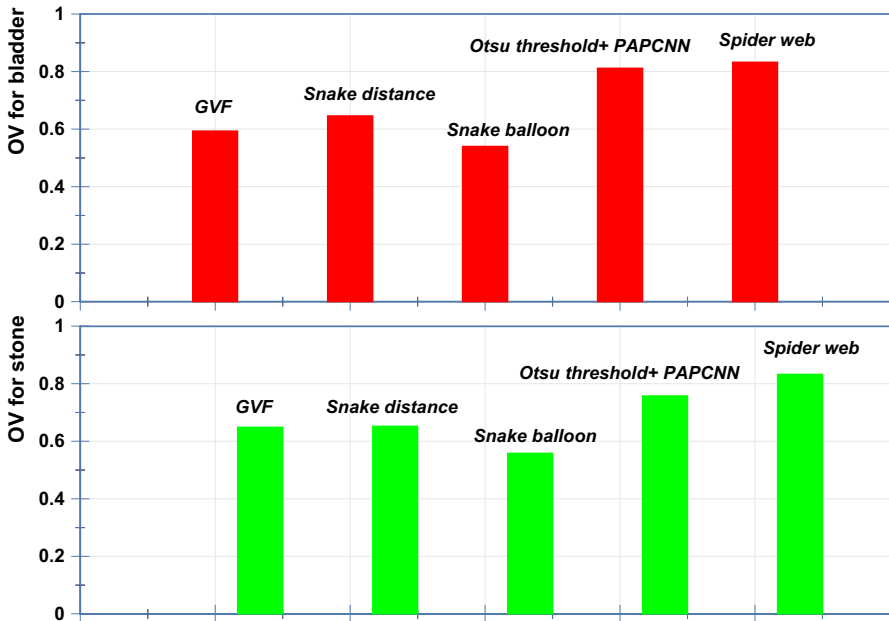


Fig. 18 Comparison of parameters for images with gallstones

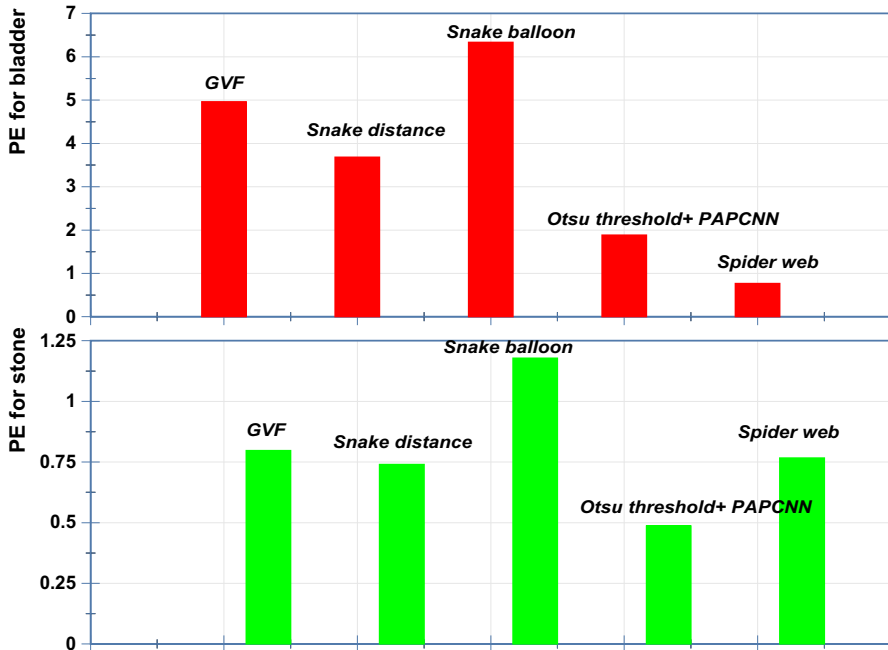


Fig. 19 Comparison of PE for images with gallstones

Table 1 Performance parameters computed for images with gallstones and with no any lesions

Image	DSC		OF		OV		PE	
	Bladder region	Stone region	Bladder region	Stone region	Bladder region	Stone region	Bladder region	Stone region
<i>Image with gallstones (input set 1)</i>								
1	0.9554	0.9554	0.8884	0.8884	0.8213	0.8213	0.8549	0.8549
2	0.9569	0.9569	0.8349	0.8349	0.8345	0.8345	0.8879	0.8879
3	0.9494	0.9494	0.8140	0.8140	0.8289	0.8289	0.9074	0.9074
4	0.9485	0.9485	0.8150	0.8150	0.8325	0.8325	0.8415	0.8415
5	0.9285	0.9285	0.8727	0.8727	0.8345	0.8345	0.8512	0.8512
6	0.9025	0.9025	0.8581	0.8581	0.8345	0.8345	0.8018	0.8018
7	0.8793	0.8793	0.8247	0.8247	0.8345	0.8345	0.7289	0.7289
Mean	0.9315	0.9315	0.843971	0.843971	0.831529	0.831529	0.839086	0.839086
<i>Image with no lesions (input set 2)</i>								
1	0.7432		0.7521		0.7298		0.7477	
2	0.9078		0.8134		0.8345		0.8461	

Table 1 continued

Image	DSC		OF		OV		PE	
	Bladder region	Stone region	Bladder region	Stone region	Bladder region	Stone region	Bladder region	Stone region
3	0.7651		0.8451		0.8345		0.8035	
4	0.874		0.8385		0.81712		0.81421	
5	0.9094		0.8576		0.8345		0.8824	
6	0.8732		0.8386		0.81711		0.8152	
7	0.9848		0.8195		0.8345		0.8292	
8	0.9287		0.9457		0.8345		0.8461	
Mean	0.873167		0.8389		0.81705		0.81452	

Table 2 Comparison of parameters for images with gallstones (input set 1) and with no any lesions (input set 2)

Method	DSC		OF		OV		PE	
	No lesions	With stones	No lesions	With stones	No lesions	With stones	No lesions	With stones
ME	0.8020	0.8273	0.7704	0.7907	0.7682	0.7844	2.8670	2.7708
MO	0.7804	0.7913	0.7336	0.7533	0.7201	0.7441	2.0992	1.6442
Spider method	0.873167	0.9315	0.8389	0.843971	0.81705	0.831529	0.81452	0.839086

5 Conclusion

Accurate segmentation of gallbladder and gallstone from the ultrasound scan image is a difficult task. In this paper, a biologically inspired algorithm is presented for the automatic segmentation of gallbladder and gallstones. Biologically inspired algorithms are developed from the behavior of a certain species. The construction of spider web by the spider is adopted in this work, and the segmentation algorithm based on spider web construction is proposed. This method accurately segments the gallbladder and gallstone regions from the image, by searching image pixels based on the intensity. To determine the characteristics of lesions presenting in the gallbladder accurately, an efficient noise filter is employed in this work. The performance metrics such as dice similarity coefficient (DSC), overlap function (OF), overlap value (OV) and position error (PE) are evaluated and compared with the other state-of-the-art methods. The values of parameters such as DSC, OF and OV are larger than those obtained in previous works and position error is less which is equal to 0.81452. From the comparative analysis, it is observed that the segmented region in the proposed method is similar to the original region. As a future part of this work, classifier will be applied to detect polyps, lithiasis, gallstone along with the detection of gallbladder.

Table 3 Comparison of parameters for images with gallstones (input set 1)

Method	DSC		OF		OV		PE	
	Gallbladder	Gallstones	Gallbladder	Gallstones	Gallbladder	Gallstones	Gallbladder	Gallstones
GVF	0.891	0.778	0.6059	0.7583	0.5932	0.6485	4.9609	0.7976
Snake distance	0.7721	0.7743	0.6650	0.6959	0.6462	0.6521	3.6827	0.7402
Snake balloon	0.6964	0.7044	0.7095	0.8035	0.5398	0.5581	6.3337	1.1778
Otsu threshold + PAPCNN	0.8938	0.8604	0.8540	0.8494	0.8114	0.7575	1.8839	0.4868
Spider web	0.9315	0.9315	0.843971	0.843971	0.831529	0.831529	0.839086	0.839086

Table 4 Comparison of performance of various filters

Method	DSC		OF		OV		PE	
	Gallbladder	Gallstones	Gallbladder	Gallstones	Gallbladder	Gallstones	Gallbladder	Gallstones
Moving average filter	0.9102	0.8327	0.8789	0.8212	0.8091	0.8021	0.8333	0.8122
Gaussian filter	0.8921	0.9012	0.8812	0.8338	0.8444	0.80912	0.8912	0.8012
Sobel filter	0.9045	0.8768	0.8122	0.8989	0.8001	0.8012	0.8821	0.8321
Spider web + DooG filter	0.9315	0.9315	0.8439	0.8439	0.8315	0.8315	0.8390	0.8390

Acknowledgements The authors thank Dr. P. Vijay Babu, MBBS, DMRD, Consultant Radiologist, Vijay Scans, Rajapalayam, Tamil Nadu, for supporting the research by providing Ultrasound images and necessary patient information. The author would like to thank the management of Kalasalingam University for providing financial assistance under the University Research Fellowship. Also we thank the Department of Electronics and Communication Engineering of Kalasalingam University, Tamil Nadu, India, for permitting to use the computational facilities available in Centre for Research in Signal Processing and VLSI Design which was set up with the support of the Department of Science and Technology (DST), New Delhi, under FIST Program in 2013 (Reference No. SR/FST/ETI-336/2013 dated November 2013).

Compliance with ethical standards

Conflict of interest Both authors declare that they have no conflict of interest.

References

1. Caselles V, Kimmel R, Sapiro G (1997) Geodesic active contours. *Int J Comput Vision* 22:61. <https://doi.org/10.1023/A:1007979827043>
2. Kass M, Witkin A, Terzopoulos D (1988) Snakes: active contour models. *Int J Comput Vision* 1:321. <https://doi.org/10.1007/BF00133570>
3. Kichenassamy S, Kumar A, Olver P et al (1996) Conformal curvature flows: from phase transitions to active vision. *Arch Ration Mech Anal* 134:275. <https://doi.org/10.1007/BF00379537>
4. Cohen LD (1991) On active contour models and balloons. In: *CVGIP: Image Understanding*, vol 53(2), pp 211–218. ISSN 1049-9660. [https://doi.org/10.1016/1049-9660\(91\)90028-N](https://doi.org/10.1016/1049-9660(91)90028-N). <http://www.sciencedirect.com/science/article/pii/S04996609190028N>
5. Yezzi A, Tsai A, Willsky A (1999) A statistical approach to snakes for bimodal and trimodal imagery. In: *The Proceedings of the 7th IEEE International Conference on Computer Vision*, vol 2. IEEE. <https://doi.org/10.1109/ICCV.1999.790317>
6. Nakhmani A, Tannenbaum A (2012) Self-crossing detection and location for parametric active contours. *IEEE Trans Image Process*. <https://doi.org/10.1109/TIP.2012.2188808>
7. Piotr Makowski P, Sorensen TS, Therkildsen SV, Materka A, Jorgensen HS, Pedersen EM (2002) Two-phase active contour method for semiautomatic segmentation of the heart and blood vessels from MRI images for 3D visualization. *Comput Med Imaging Graph* 26(1), pp 9–17. ISSN 0895-6111. [https://doi.org/10.1016/S0895-6111\(01\)00026-X](https://doi.org/10.1016/S0895-6111(01)00026-X). <http://www.sciencedirect.com/science/article/pii/S089561110100026X>
8. Bodzioch S, Ogiela MR (2009) New approach to gallbladder ultrasonic images analysis and lesions recognition. *Comput Med Imaging Graph* 33(2):154–170. <https://doi.org/10.1016/j.compmedimag.2008.11.003>
9. Ciecholewski M (2010) Gallbladder boundary segmentation from ultrasound images using active contour model. In: Fyfe C, Tino P, Charles D, Garcia-Osorio C, Yin H (eds) *Intelligent data engineering and automated learning—IDEAL 2010*. IDEAL 2010. Lecture notes in computer science, vol 6283. Springer, Berlin
10. Ciecholewski M (2011) Ada boost-based approach for detecting lithiasis and polyps in USG images of the gallbladder. In: Badioze Zaman H et al (eds) *Visual informatics: sustaining research and innovations. IVIC 2011*. Lecture notes in computer science, vol 7066. Springer, Berlin
11. Ciecholewski M, Chochołowicz J (2013) Gallbladder shape extraction from ultrasound images using active contour models. *Comput Biol Med* 43(12):2238–2255. <https://doi.org/10.1016/j.compbiomed.2013.10.009>
12. Lian J, Ma Y et al (2017) Automatic gallbladder and gallstone regions segmentation in ultrasound image. *Int J CARS* 12(4):553–568. <https://doi.org/10.1007/s11548-016-1515-z>
13. Xie W et al (2013) Gallstone segmentation and extraction from ultrasound images using level set model. In: *Biosignals and Biorobotics Conference (BRC), 2013* ISSNIP. IEEE
14. Obadia BL, Gee A (1999) Adaptive segmentation of ultrasound images. *Image Vis Comput* 17(8):583–588. [https://doi.org/10.1016/S0262-8856\(98\)00177-2](https://doi.org/10.1016/S0262-8856(98)00177-2) ISSN 0262-8856
15. Wimmer A, Soza G, Hornegger J (2009) A generic probabilistic active shape model for organ segmentation. In: Yang GZ, Hawkes D, Rueckert D, Noble A, Taylor C (eds) *Medical image computing and*

- computer-assisted intervention—MICCAI 2009. MICCAI 2009. Lecture notes in computer science, vol 5762. Springer, Berlin
16. Abolmaesumi P, Sirouspour MR (2004) An interacting multiple model probabilistic data association filter for cavity boundary extraction from ultrasound images. *IEEE Trans Med Imaging* 23(6):772–784
 17. Gloger O et al (2017) Automatic gallbladder segmentation using combined 2D and 3D shape features to perform volumetric analysis in native and secretin-enhanced MRCP sequences. *Magn Reson Mater Phys Biol Med* 2017:1–15
 18. Saito A, Nawano S, Shimizu A (2017) Fast approximation for joint optimization of segmentation, shape, and location priors, and its application in gallbladder segmentation. *Int J CARS* 12:743. <https://doi.org/10.1007/s11548-017-1571-z>
 19. Arunkumar N, Ramkumar K, Venkatraman V, Abdulhay E, Fernandes SL, Kadry S, Segal S (2017) Classification of focal and non focal EEG using entropies. *Pattern Recognit Lett* 94:112–117
 20. Arunkumar N, Kumar KR, Venkataraman V (2016) Automatic detection of epileptic seizures using new entropy measures. *J Med Imaging Health Inform* 6(3):724–730
 21. Fernandes SL, Gurupur VP, Sunder NR, Arunkumar N, Kadry SA (2017) Novel noninvasive decision support approach for heart rate measurement. *Pattern Recognit Lett*. <https://doi.org/10.1016/j.patrec.2017.07.002>
 22. Hamza R, Muhammad K, Arunkumar N (2017) González GR (2017) Hash based encryption for keyframes of diagnostic hysteroscopy. *IEEE Access*, New York
 23. Kennedy J, Eberhart RC (1995) Particle swarm optimization. In: *Proceedings of IEEE International Conference on Neural Networks (Perth, Australia)*, vol 5(3). IEEE Service Center, Piscataway, pp 1942–1948
 24. Dorigo M, Birattari M, Stutzle T (2006) Ant colony optimization. *IEEE Comput Intell Mag* 1(4):28–39
 25. Abbass HA (2001) MBO: marriage in honey bees optimization—a haplometrosis polygynous swarming approach. In: *Proceedings of the 2001 Congress on Evolutionary Computation*, vol 1. IEEE
 26. Martin R, Stephen W (2006) Termite: a swarm intelligent routing algorithm for mobile wireless ad-hoc networks. In: *Stigmergic Optimization. Studies in Computational Intelligence*, vol 31. Springer, Berlin, pp 155–184
 27. Neshat M, Sepidnam G, Sargolzaei M et al (2014) Artificial fish swarm algorithm: a survey of the state-of-the-art, hybridization, combinatorial and indicative applications. *Artif Intell Rev* 42:965–997. <https://doi.org/10.1007/s10462-012-9342-2>
 28. Mucherino A, Seref O (2007) Monkey search: a novel metaheuristic search for global optimization. In: *AIP Conference Proceedings*, vol 953(1). AIP
 29. Yang XS, Deb S (2009) Cuckoo search via levy flights. In: *2009 World Congress on Nature and Biologically Inspired Computing (NaBIC)*, Coimbatore, pp 210–214. <https://doi.org/10.1109/NABIC.2009.5393690>
 30. Yang XS (2010) Firefly algorithm, stochastic test functions and design optimisation. *Int J Bio-Inspir Comput* 2(2):78–84
 31. Mirjalili S, Mirjalili SM, Lewis A (2014) Grey wolf optimizer. In: *Advances in Engineering Software*, vol 69, pp 46–61. ISSN 0965-9978. <https://doi.org/10.1016/j.advengsoft.2013.12.007>. <http://www.sciencedirect.com/science/article/pii/S0965997813001853>
 32. Yazdani M, Jolai F (2016) Lion optimization algorithm (LOA): a nature-inspired metaheuristic algorithm. *J Comput Des Eng* 3(1): 24–36. ISSN 2288-4300. <https://doi.org/10.1016/j.jcde.2015.06.003>. <http://www.sciencedirect.com/science/article/pii/S2288430015000524>
 33. Li C, Duan H (2014) Target detection approach for UAVs via improved pigeon-inspired optimization and edge potential function. In: *Aerospace Science and Technology*, vol 39, pp 352–360. ISSN 1270-9638. <https://doi.org/10.1016/j.ast.2014.10.007>. <http://www.sciencedirect.com/science/article/pii/S1270963814002053>
 34. Mirjalili S, Lewis A (2016) The whale optimization algorithm. In: *Advances in engineering software*, vol 95, pp 51–67. ISSN 0965-9978. <https://doi.org/10.1016/j.advengsoft.2016.01.008>. <http://www.sciencedirect.com/science/article/pii/S0965997816300163>
 35. Mirjalili S (2016) Dragonfly algorithm: a new meta-heuristic optimization technique for solving single-objective, discrete, and multi-objective problems. *Neural Comput Appl* 27:1053. <https://doi.org/10.1007/s00521-015-1920-1>
 36. Sanz SS, Del Ser J, Torres IL, Lopez SG, Figueras JAP (2014) The coral reefs optimization algorithm: a novel metaheuristic for efficiently solving optimization problems. *Sci World J*, 15 pages. Article ID 739768. <https://doi.org/10.1155/2014/739768>

37. Yu JJQ, Li VOK (2016) A social spider algorithm for solving the non-convex economic load dispatch problem. In: *Neurocomputing*, vol 171, pp 955–965. ISSN 0925-2312. <https://doi.org/10.1016/j.neucom.2015.07.037>. <http://www.sciencedirect.com/science/article/pii/S0925231215010188>
38. Liu Z et al (2016) A new search algorithm of MBD based on spider web and its application in power distribution network fault diagnosis. *Int J Artif Intell Tools* 25(02):1650002
39. Anter AM, Hassanien AE, ElSoud MA, Kim TH (2015) Feature selection approach based on social spider algorithm: case study on abdominal CT liver tumor. In: 2015 7th International Conference on Advanced Communication and Networking (ACN), Kota Kinabalu, pp 89–94. <https://doi.org/10.1109/ACN.2015.32>
40. Ouadfel S, Ahmed AT (2016) Social spiders optimization and flower pollination algorithm for multilevel image thresholding: a performance study. In: *Expert Systems with Applications*, vol 55, pp 566–584. ISSN 0957-4174. <https://doi.org/10.1016/j.eswa.2016.02.024>
41. Muneeswaran V, Rajasekaran MP (2018) Beltrami-regularized denoising filter based on tree seed optimization algorithm: an ultrasound image application. In: Satapathy S, Joshi A (eds) *Information and communication technology for intelligent systems (ICTIS 2017)—volume 1*. ICTIS 2017. Smart innovation, systems and technologies, vol 83. Springer, Cham. https://doi.org/10.1007/978-3-319-63673-3_54
42. Muneeswaran V, Rajasekaran MP (2017) Analysis of particle swarm optimization based 2D FIR filter for reduction of additive and multiplicative noise in images. In: Arumugam S, Bagga J, Beineke L, Panda B (eds) *Theoretical computer science and discrete mathematics*. ICTCSDM 2016. Lecture notes in computer science, vol 10398. Springer, Cham. https://doi.org/10.1007/978-3-319-64419-6_22
43. Abdel-Basset M, El-Shahat D, Sangaiah AK (2017) A modified nature inspired meta-heuristic whale optimization algorithm for solving 0–1 knapsack problem. *Int J Mach Learn Cybern*. <https://doi.org/10.1007/s13042-017-0731-3>
44. Abdel-Basset M, Fakhry AE, El-henawy I, Qiu T, Sangaiah AK (2017) Feature and intensity based medical image registration using particle swarm optimization. *J Med Syst* 41(12):197. <https://doi.org/10.1007/s10916-017-0846-9>
45. Abdel-Basset M, Shawky LA, Sangaiah AK (2017) A comparative study of cuckoo search and flower pollination algorithm on solving global optimization problems. *Libr Hi Tech*. <https://doi.org/10.1108/LHT-04-2017-0077>
46. Firdaus A, Anuar NB, Ab Razak MF, Sangaiah AK (2017) Bio-inspired computational paradigm for feature investigation and malware detection: interactive analytics. *Multimed Tools Appl*. <https://doi.org/10.1007/s11042-017-4586-0>
47. Goyal RK, Kaushal S, Sangaiah AK (2017) The utility based non-linear fuzzy AHP optimization model for network selection in heterogeneous wireless networks. *Appl Soft Comput*. <https://doi.org/10.1016/j.asoc.2017.05.026>